Available online at www.sciencedirect.com

SCIENCE DIRECT®

Journal of Catalysis 231 (2005) 443–452

JOURNAL OF CATALYSIS

www.elsevier.com/locate/jcat

Catalytic activity of synthetic saponite clays: effects of tetrahedral and octahedral composition

R.J.M.J. Vogels [a], J.T. Kloprogge [b,*], J.W. Geus [c]

[a] *Philips Lighting B.V., Frontstraat 4, 5405 AK, Uden, the Netherlands*
[b] *Inorganic Materials Research Program, School of Physical and Chemical Sciences, Queensland University of Technology,*
GPO Box 2434, Brisbane, Qld 4001, Australia
[c] *Department of Inorganic Chemistry, Utrecht University, PO Box 80083, 3508 TB, Utrecht, the Netherlands*

Received 27 September 2004; revised 31 January 2005; accepted 3 February 2005

Abstract

This paper describes the catalytic characteristics of synthetic saponites with well-known chemical composition, thermal stability, and acidity in three catalytic reactions: (1) catalytic cracking of n-dodecane, (2) hydro-isomerisation of n-heptane, and (3) Friedel–Crafts alkylation of benzene. Saponites with Mg in the octahedral position were by far the best catalysts for the catalytic cracking of n-dodecane, which can be explained by the higher surface area of these saponites compared with saponites with other compositions. All saponites performed better in the hydro-isomerisation reaction of n-heptane and Friedel–Crafts alkylation compared with commercially available catalysts such as HZSM-5 and ASA. The shape selectivity in the Friedel–Crafts alkylation of benzene for p- and o-DIOPB was remarkably high for the synthetic saponites.

Keywords: Clay; Saponite; Catalytic cracking; Friedel–Crafts alkylation; Hydro-isomerisation; Selectivity

1. Introduction

The first recorded catalytic application of clay minerals was due to Bondt et al., who investigated the dehydration of alcohol in 1797 [1] (mentioned by [2]). Since that time clay minerals have been used in a large variety of catalytic reactions. In the beginning of this century mainly the clay mineral palygorskite was employed in isomerisation, oxidation, and polymerisation reactions [3]. The main breakthrough of clay minerals in catalysis was the use of clays in catalytic cracking. Although this application was known for some years, Houdry solved the problem of catalyst regeneration in the early 1930s, resulting in industrial processes with clay minerals [4]. Hettinger [2] published a good review about Houdry's development of clay minerals as cracking catalysts. Up to about 1955 the use of (acid-activated) clay minerals, such as montmorillonite and halloysite, in catalytic cracking increased. Subsequently the clay minerals were replaced, however, by amorphous silica-aluminas followed by zeolites in the early 1960s.

Clay minerals, such as kaolinite, are still used in the matrix of cracking catalysts [2]. Since the late 1970s developments concerning clays pillared with inorganic complexes has renewed interest in the application of clay minerals as cracking catalysts (e.g., [5–9]). For a long time hydro-isomerisation has also frequently been executed with clay minerals (e.g., [10]). Later, work on synthetic mica-montmorillonites with transition metals in the octahedral sheet became important for hydro-isomerisation reactions [11–13]. Recently, synthetic pillared Ni-substituted saponites have been developed for hydro-isomerisation purposes [14]. In addition to catalytic cracking and (hydro)-isomerisation, clay minerals have been used in many other catalytic processes, such as (de)hydration, dimerisation,

---

[*] Corresponding author. Fax: +61 3864 1804.
E-mail address: t.kloprogge@qut.edu.au (J.T. Kloprogge).

0021-9517/$ – see front matter
doi:10.1016/j.jcat.2005.02.004

polymerisation, disproportionation, hydrolysis, oxidation, desulphurisation, (de)hydrogenation, hydroformulation, Diels–Alder reactions, epoxidation, alkylation, acylation, and ester formation. Many of these reactions are frequently reviewed in detail (e.g., [3,9,15–17]).

Studies on the use of clay minerals, in place of hazardous homogeneous catalysts, in liquid-phase reactions for the production of fine chemicals are receiving much attention now. Generally four types of clay minerals are used:

(1) "Normal" smectite clays with acid sites generated by isomorphous substitution in the tetrahedral or octahedral sheets. Montmorillonite clays are most frequently used. The catalytic activity can be enhanced by replacement of the interlayer cations (usually Na^+, Ca^{2+}) with acidic cations, such as H^+, Al^{3+}, and Fe^{3+} [16,18,19].

(2) The catalytic properties of smectites can be enhanced by acid treatment of the smectite surface with sulphuric or hydrochloric acid to remove ions from the octahedral sheet, to increase the layer charge and the pore volume [16,20].

(3) The smectite surface is often doped with high-valence Lewis acids, such as Fe^{3+}-chloride [21,22], or with metallic nitrates [23] to increase the performance in acid-catalysed reactions. Leaching of the loaded material has been observed, however [24].

(4) Organometallic compounds, such as metal chelate complexes [25], or inorganic polyoxocationic pillars [8,9,15] have often been intercalated to increase the acidity and/or the specific surface area, which results in an increase of the catalytic performance.

The majority of the catalytic reactions using clays are performed with natural clay minerals. To enhance the acidic properties of these clays, the above-mentioned modifications 2, 3, and 4 are applied, but these methods do not circumvent the disadvantages of the natural materials with respect to the relatively low and uncontrollable specific surface area and pore volume, the presence of impurities, and the variable chemical composition. Synthetic clays are scarcely used in these organic reactions [26,27], probably because of the high cost involved in their hydrothermal preparation. The textural and acidic characteristics of synthetic saponites [28–30] indicate that the above-mentioned disadvantages can be avoided. The objective of this paper is to assess whether the synthetic saponites are active in acid-catalysed reactions. Therefore, some introductory catalytic tests have been performed with three different kinds of acid-catalysed reactions. The test reactions involve the catalytic cracking of n-dodecane, the hydro-isomerisation of n-heptane, and the alkylation of benzene with propylene to cumene. From the results of the application of the synthetic saponites in these reactions, we will try to establish a relation between the acidity as described by [30] and the texture [28,29] and the corresponding catalytic performance.

2. Experimental

2.1. Saponite synthesis

Synthetic saponites were prepared according to the method described by Vogels et al. [28]. All synthesis procedures were performed with stoichiometric amounts of the chemicals listed in the next paragraphs corresponding to the desired products, that is, saponite. The theoretical composition of saponite is $N_{x/z}{}^{z+}[M_6][Si_{8-x}Al_x]O_{20}(OH)_4 \cdot nH_2O$ and $[M_6][Si_8O_{20}](OH)_4$, respectively. M and N correspond to the divalent octahedral and the interlayer cation, respectively. The type of octahedral cation, M, will be used as a prefix before the mineral name. For instance, saponites with Mg^{2+} as an octahedral cation will be further denoted as Mg-saponite. Ni^{2+}, Mg^{2+}, Zn^{2+}, and Co^{2+} have been used as the cations in the octahedral sheets. The Si/Al ratio has been varied between 5.67–39.0, 2.33–39.0, and 7.89–39.0, with Mg^{2+}-, Zn^{2+}-, and Co^{2+}-saponites, respectively. $NH_4{}^+$-saponite has only been used with a Si/Al ratio of 7.89.

All experiments were carried out in a double-walled Pyrex vessel equipped with stirrer and baffles to ensure homogeneity of the contained mixture [31]. We maintained the temperature during the synthesis at 90 °C by circulating thermostat-controlled water between the inner and outer walls of the vessel. A Si/Al gel with a Si/Al molar ratio of 5.67 ($x = 1.2$) was prepared according to the following procedure: 40 g of a Na_2SiO_3 solution (27 wt% SiO_2) was diluted by the addition of 100 ml demineralised water. We prepared an $Al(OH)_4{}^-$ solution by dissolving 11.9 g $Al(NO_3)_3 \cdot 9H_2O$ in 80 ml of a 2 M NaOH solution. The Al-containing solution was gradually added to the Si-containing solution under continuous stirring within approximately 30 s, after which the initially clear solution became cloudy and hardened to a gel. At this point the stirring was stopped and the mixture was allowed to stand for 1 h before further use. The gels did not contain excess liquid and were not treated before further use. We prepared gels with Si/Al molar ratios of 7.89 ($x = 0.9$) and 12.3 ($x = 0.6$) in a comparable manner by adjusting the amounts of aluminium nitrate and sodium silicate. The total amount of Si + Al was kept constant. A gel with a Si/Al ratio of 39.0 ($x = 0.2$) was prepared in a slightly different way, because after we mixed the Si- and Al-containing solutions together, no gelation proceeded. After the addition of 10 ml HNO_3 (65%), however, a stable white gel resulted. Gels with an exceptionally low Si/Al ratio of 2.33 ($x = 2.4$) were prepared in a manner similar to those of the other Si/Al gels, but without the addition of NaOH in the Al-containing solutions. This had to be done to reduce the rate of gelation.

The final gel was put into the above vessel together with 1000 ml of demineralised water and heated to 90 °C. The required amount of $Mg(NO_3)_2 \cdot 6H_2O$, $Ni(NO_3)_2 \cdot 6H_2O$, $Zn(NO_3)_2 \cdot 4H_2O$, $Co(NO_3)_2 \cdot 6H_2O$, and typically 36.0 g urea was dissolved in 500 ml of water and subsequently added to the gel–water mixture kept at 90 °C, after which the synthesis procedure started. Addition of the above solution resulted in a decrease in the temperature of the synthesis mixture of approximately 10 °C. No acidification of the synthesis mixture was executed before the start of the synthesis procedure because the gels were not stable in the acidified solutions. We prepared saponites with octahedral sheets consisting of two metals by using the desired combination of the divalent metal nitrate salts in the synthesis mixture. The ratio between the two cations in the octahedral sheets was varied between 1 and 29. One series of experiments concerning the preparation of Zn-saponite was executed with variable amounts of urea to investigate the effect of the concentration of the hydrolysing urea on the saponite formation. The amounts of urea in the starting mixture were 0.0, 18.0, and 72.1 g. An additional synthesis was performed with 36.0 g urea and additional NaOH, which raised the pH to 8 in the initial mixture.

The synthesis duration was kept constant at 20 h unless mentioned otherwise. After the desired period of time of synthesis the cloudy suspensions were filtered. The white (Zn, Mg), light green (Ni), and pink (Co) filtrates were washed thoroughly with demineralised water and dried overnight at 130 °C before use. All samples were NH_4^+ exchanged. Before each measurement the saponites were calcined at 450 °C for 1 h in a N_2 flow, resulting in the deammoniation of the saponites with H^+ as the remaining charge-compensating cation.

2.2. Catalytic cracking of *n*-dodecane

Catalytic measurements were performed in a fixed-bed nanoflow pulse unit of the Koninklijke/Shell Laboratorium Amsterdam (KSLA, now known as SRTCA, Shell Research and Technology Centre Amsterdam). The applied reaction conditions were 450 °C at 4 bar total pressure. The composition of the pulsed gas flow was helium, *n*-dodecane, and nitrogen at concentrations of 19.5, 12.5, and 67.9 mol%, respectively. The catalyst bed consisted of 20 wt% synthetic saponite and 80 wt% silica. A sieve fraction of both solids between 0.212 and 0.300 mm was used. The WHSV (weight hourly space velocity) during the pulses was estimated to be 66 h^{-1}. The ratio of *n*-dodecane/catalyst of each pulse was 0.18 g/g. After each pulse the catalyst bed was kept at 450 °C under an inert gas flow for approximately 1 h. The products were analysed with a gas chromatograph. He (as tracer gas) and H_2 were detected with a thermal conductivity detector (TCD) followed by the analysis of the hydrocarbons C_1 up to and including C_5. The hydrocarbons C_6–C_{12} were measured in one backflush peak. The catalyst activity is expressed as the first-order reaction rate constant k: $k = [-\ln(1 - 0.01(C_5\text{-yield}))]/[\text{ct} \cdot \text{cf}]$, where C_5-yield, ct, and cf correspond to the total amount of C_1 to C_5, the contact time, and the catalyst fraction, respectively. The assumption of a first-order reaction with this experimental setup agrees with the results of Corma et al. [32]. For reasons of comparison, the catalytic activities of a "fresh" zeolite Y and of an equilibrated zeolite Y from a cracking unit (E-Y) have been included in our study.

2.3. Hydro-isomerisation of *n*-heptane

The experiments were executed in a catalytic test unit of the SRTCA. All reactions were performed in a fixed-bed reactor at a total pressure of 30 bar. The feed consisted of *n*-heptane and hydrogen in a 1:4 mol/mol ratio. The reactions were executed with increasing and decreasing temperature between 160 and 400 °C, which was changed at a rate of 0.22 °C/min. The GHSV in all cases was 1120 ml(stp)/(g h). The products were analysed with a gas chromatograph. The activity of the catalysts is denoted as the temperature at which the conversion was 40%. All saponite samples were NH_4^+ exchanged and subsequently calcined at 450 °C for 4 h to obtain H^+ as the charge compensating cation. A sieve fraction of 40–80 mesh was used. This fraction was impregnated with 0.4% Pt. Before each reaction the catalysts were reduced in situ at 400 °C for 2 h. Measurements on a commercial amorphous silica-alumina (ASA) catalyst and a typical HZSM-5 zeolite (both also loaded with 0.4% Pt) were also performed.

2.4. Friedel–Crafts alkylation of benzene with propylene to cumene

The synthetic saponites were tested for their ability to alkylate benzene with propylene to cumene (isopropylbenzene). For comparison purposes a commercial solid phosphoric acid (SPA) catalyst was also investigated. All experiments were carried out in the research laboratory of Engelhard and De Meern. A sieve fraction of the catalyst between 0.1 and 0.4 mm was taken. To avoid the introduction of water, the synthetic clays were calcined under a nitrogen flow for 3 h at a desired temperature. After the calcination, the saponites were suspended in dry benzene and transferred to a stainless-steel autoclave. To obtain information about the effect of water on the catalytic performance, a noncalcined sample and a wet sample were also measured. Propylene was introduced into the autoclave, the content of which was continuously mixed, after which the temperature was raised to the desired level. To prevent multiple alkylation, an excess of benzene was used with typical values for the benzene/propylene ratio between 7 and 8. The catalyst concentration amounted to 0.2 or 1.5 wt%. The benzene/propylene molar ratios, the type of catalyst, the reaction temperature, and the reaction duration are mentioned in the appropriate figures and tables. Analyses were performed on a Carlo Erba Instruments HRGC 5300 gas chromatograph with a capillary Chrompack CP-Sil-CB column. Unreacted propylene could not be measured. The conversion and selectivity were calculated as follows:

$$\text{Conversion} = \frac{\text{mole cumene} + 2(\text{mole DIPB}) + 3(\text{mole TIPB formed})}{\text{mole propylene in starting mixture}} \times 100\%,$$

$$\text{Selectivity} = \frac{\text{mole cumene formed}}{\text{mole cumene} + 2(\text{mole DIPB}) + 3(\text{mole TIPB formed})} \times 100\%.$$

The abbreviations DIPB and TIPB are used for diisopropylbenzene and triisopropylbenzene, respectively. The formation of n-propylbenzene and of oligomers of propylene was negligible. These compounds are, therefore, not included in the calculations.

3. Results and discussion

3.1. Catalytic cracking of *n*-dodecane

The relation between the type of octahedral cation of the saponite and the corresponding catalytic activity in the cracking reaction of n-dodecane is represented in Fig. 1. Mg-saponite displayed by far the highest initial first-order rate constant (k), followed by Co, Ni, and Zn. The k-value of a fresh zeolite Y (not displayed in Fig. 1) 37.2, is very high. The E-Y has an initial k-value of 12, which is comparable to that of Zn-saponite. The observation that the rate constant of Mg-saponite is much higher than those of the other saponites cannot be attributed simply to the more elevated specific surface area [28]. The specific surface area of Mg-saponites typically ranges from 600 to 750 m^2/g, whereas the specific surface areas of Ni-, Co-, and Zn-saponites vary between 500 and 600, 400 and 500, and 100 and 300 m^2/g, respectively. The high reaction rate constant of Mg-saponite also cannot be explained by differences in acid strength between Mg-saponite and, for instance, Zn-saponite [30]. The reducibility of the metal ions within the octahedral sheets is determining together with the specific surface area the activity in the cracking of n-dodecane. Neither Mg^{2+} nor Zn^{2+} present within the octahedral layers can be reduced by hydrogen at temperatures up to 800 °C. The specific surface area of Mg-saponite is a factor 2 to 7.5 higher than that of Zn-saponite, whereas the initial activity differs by a factor of about 9. Accordingly, the ratio of the activities, as evident from the ratio of the rate constants, cannot be completely attributed to the difference in specific surface area.

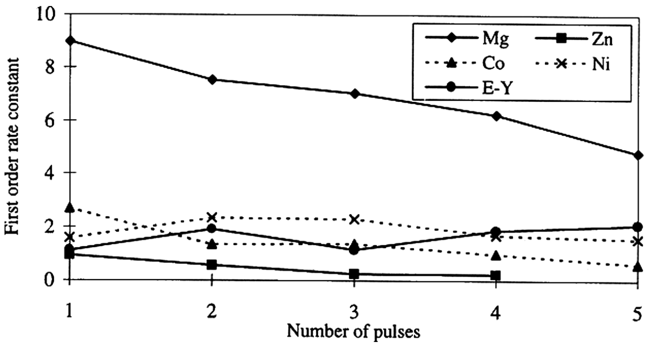

Fig. 1. The relation at 450 °C between the first-order reaction rate constant of saponites (Si/Al ratio 7.89) with different octahedral cations (Mg^{2+}, Zn^{2+}, Co^{2+}, and Ni^{2+}) and the pulse number. Zeolite E-Y has been included for reference. Feed composition: n-dodecane, N_2, He; WHSV 66 h^{-1}.

The Ni^{2+} and Co^{2+} ions within the octahedral layers are liable to reduction upon exposure to n-dodecane at 450 °C. Reduction of the metal ions of the octahedral sheets leads to a collapse of the clay structure, which leads to a loss of the acid properties. In earlier work [29] it was established that Ni^{2+} ions present within the octahedral sheets of saponites are more readily reduced than Co^{2+} ions. We therefore feel that exposure of Ni-saponite to n-dodecane at 450 °C leads to relatively large metallic nickel particles and to an extensive destruction of the clay structure. As a result, the activity of the reduced Ni-saponite is low and due mainly to the metallic nickel particles resulting from the reduction. With Co-saponite, reduction will proceed to a smaller extent. The number of acid sites will consequently drop appreciably, and metallic cobalt particles, which are due to the lower extent of reduction, will be appreciably smaller than the nickel particles within the reduced Ni-saponites. Despite the fact that the specific surface areas of the fresh Ni- and Co-saponites are not much smaller than that of Mg-saponite, their activity is much lower. According to the pyridine adsorption on W-saponites, Lewis acid sites are present almost exclusively, because of the presumed migration of W from the interlayer into the clay structure. It can thus be stated that the catalytic cracking behaviour is due mainly to Lewis acid centres with Mg- and Zn-saponites. The remaining activity of the (reduced) Ni- and Co-saponites can be due partly to the metal particles. A contribution of the metal particles will be evident from the selectivity. As can be seen in Fig. 1, the deactivation of Mg-saponite is considerable, most likely because of the formation of coke on the stronger (Lewis) acid sites. The fresh zeolite Y with strong Brønsted acid sites deactivated very rapidly according to the decrease of k from 37.2 at pulse 1 to 6.5 at pulse 5 (not displayed in Fig. 1). Deactivation of the other saponites is also observable, though it is not as pronounced as with the Mg-saponite.

The selectivities for C_1–C_5 products are listed in Tables 1 and 2. Saponites with Zn^{2+} or Mg^{2+} as the octahedral cations show a selectivity comparable to that of the E-Y. In particular, C_4 was formed during the catalytic cracking of n-dodecane on these saponites. The incorporation of Ni^{2+} into the octahedral sheet strongly influences the selectivity as compared with Mg-, Zn-saponites, and E-Y. The formation of large amounts of hydrogen and methane results in a relatively low amount of C_3, C_4, and C_5 in the reaction products. The formation of hydrogen and methane clearly points to the presence of metallic nickel particles. As was indicated already by the rate constant, nickel ions within the

Table 1
Selectivity (wt%) of the C_1–C_5 fraction produced in the cracking of *n*-dodecane. All saponite samples have a Si/Al ratio = 7.89

Product[a] (wt%)	Mg-sap.	Zn-sap.	Ni-sap.	Co-sap.	Zeolite-Y	E-Y
k	8.99	0.93	1.59	2.69	37.2	1.12
H_2	0	0	7.68	0.72	0	0
C_1	0	0	25.8	0	0.07	0
C_2	0	0	1.85	0	0.18	0
$C_2^=$	0.38	0	0	0.72	1.03	0
C_3	7.68	7.96	1.99	3.94	15.5	2.72
$C_3^=$	14.6	20.6	9.40	17.4	2.83	18.3
n-C_4	7.47	7.10	1.85	4.50	12.1	7.07
i-C_4	14.8	13.5	2.38	6.83	36.7	16.1
$C_4^=$	23.2	31.0	32.3	34.6	1.58	29.5
n-C_5	3.60	5.16	0	2.25	4.07	3.62
i-C_5	13.3	8.39	1.06	4.98	25.3	14.7
$C_5^=$	14.9	6.24	15.6	24.0	0.61	7.97
$\sum C_3$-total	22.3	28.6	11.4	21.3	18.3	21.0
$\sum C_4$-total	45.5	51.6	36.5	45.9	50.4	52.7
$\sum C_5$-total	31.8	19.8	16.7	31.2	30.0	22.7

[a] k = rate constant, C = paraffin, $C^=$ = olefin, i = iso, n = normal, total = total amount of olefins and paraffins.

Table 2
Selectivity expressed in product ratios for the cracking of *n*-dodecane[a]

Sample	Si/Al	$C_3^=$/ C_3-total	i-C_4/ $i+n$-C_4	$C_4^=$/ C_4-total	i-C_5/ $i+n$-C_5	$C_5^=$/ C_5-total
Mg-sap.	7.89	0.66	0.67	0.51	0.79	0.47
Zn-sap.	7.89	0.72	0.66	0.60	0.62	1.00
Ni-sap.	7.89	0.82	0.56	0.88	1.00	0.94
Co-sap.	7.89	0.82	0.60	0.75	0.69	0.77
Co-sap.	12.3	0.96	0.65	0.93	–	1.00
Co-sap.	39.0	1.00	–	1.00	–	1.00
E-Y	–	0.87	0.70	0.56	0.80	0.30
Zeolite Y	–	0.15	0.75	0.03	0.86	0.02

[a] k = rate constant, C = paraffin, $C^=$ = olefin, i = iso, n = normal, total = total amount of olefins and paraffins.

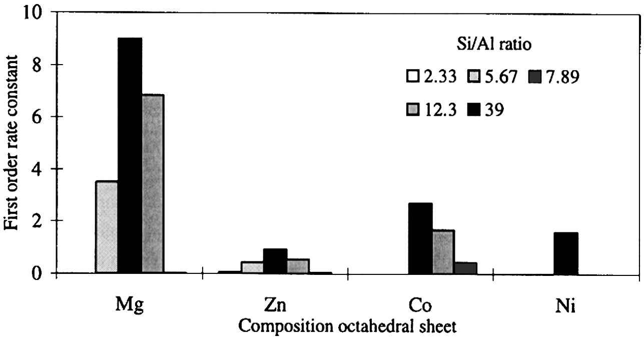

Fig. 2. The influence of the Si/Al ratio on the catalytic activity of Mg-, Zn-, Ni-, and Co-saponites. All activities were obtained in the first pulse.

octahedral sheets are reduced by the hydrocarbon in the feed. The production of hydrogen points to carbon deposition on the nickel particles. The reaction of hydrogen released with carbon leads to methane. With (reduced) Ni-saponite the production of C_2 and C_3 is relatively low, whereas much butene and pentene results. The selectivity of samples containing cobalt is also remarkable. (Reduced) Co-saponites show a very high selectivity for C_3-, C_4-, and C_5-olefins, most likely because of the dehydrogenating effect of the metallic particles. Since the metallic cobalt particles remain relatively small, carbon deposition on the metal does not proceed rapidly. Consequently, methane and hydrogen are not observed in significant amounts. A similar observation was mentioned by Meusinger et al. [33] for the cracking of *n*-hexane over Co-containing aluminium phosphate-based molecular sieves. (Reduced) Co-saponites, but probably also Ni-saponites, may exhibit a bifunctional catalytic behaviour: catalytic cracking by the acid sites and dehydrogenation by the transition metals at the clay surfaces. Although the Si/Al ratio in Mg- and Zn-saponites does not influence the selectivity appreciably (not displayed in Tables 1 and 2), the Co-saponite with a low amount of Al (Si/Al = 12.3) exhibits an extremely high dehydrogenation activity, whereas the cracking activity is low ($k = 1.68$), which confirms this bifunctionality (Table 2).

Although an influence of the Si/Al ratio on the selectivity for C_1–C_5 has been detected only for Co-saponites, the effect of the Si/Al ratio on the catalytic activity can clearly be seen with the Mg-, Zn-, and Co-saponites (Fig. 2). In Mg- and Zn-saponites an optimum in activity is observed for samples with a Si/Al ratio of 7.89. For the three measured Co-saponites, the sample with a Si/Al ratio of 7.89 displays the highest activity. These findings are in accordance with the results presented by Vogels et al. [28–30] and can be explained by the next nearest neighbour (NNN) theory for clay minerals. This NNN theory has been developed for zeolites [34–36] and implies that the acid strength of the tetrahedral Si/Al lattice in zeolites is not affected as long as an Al^{3+} ion does not have another Al^{3+}, but only Si^{4+} as NNN. An increase of the Si/Al ratio will result in the presence of Al^{3+} in NNN positions, which lowers the acid strength of the zeolite lattice. Application of this theory to saponites results in a maximum NNN situation with a Si/Al ratio of approximately 7, close to the observed maximum activity of samples with a Si/Al ratio of 7.89. It is interesting to note that with the saponites the NNN theory satisfactorily accounts for the acidity of Lewis acid sites.

3.2. Hydro-isomerisation of *n*-heptane

All synthetic saponite samples used in this study were H^+ exchanged. The results presented by Vogels et al. [30] clearly revealed the almost exclusive presence of Lewis acid sites within thus exchanged clays. The acid-catalysed isomerisation reactions on the saponites to be presented below must therefore be related to the Lewis acidity. The *n*-heptane conversion and the selectivity for *i*-heptane, presented as the yield of *i*-heptane (i-C_7 yield), as a function of temperature for an ASA, a Co- and a Mg-saponite sample, are represented in Figs. 3 and 4. The conversions and selectivities were measured while the temperature was raised. The conversion measured with the Co-saponite is considerably

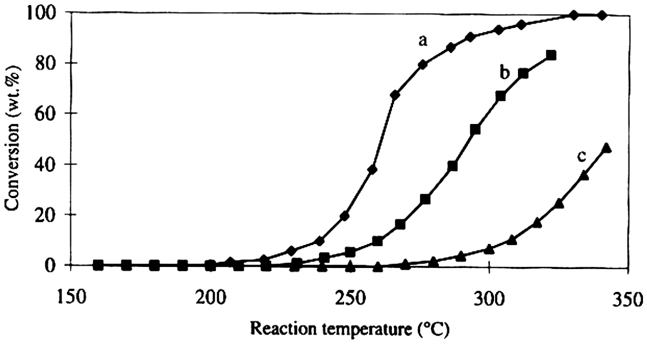

Fig. 3. The conversion of *n*-heptane at rising reaction temperatures of (a) Co-saponite (Si/Al ratio 7.89), (b) Mg-saponite (Si/Al ratio 7.89), and (c) ASA.

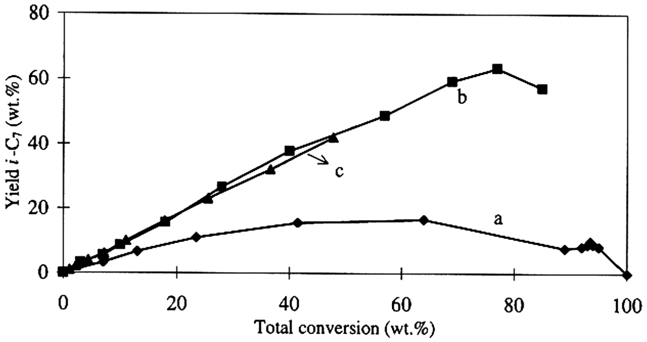

Fig. 4. The yield towards *i*-heptane as a function of the *n*-heptane conversion of (a) Co-saponite (Si/Al ratio 7.89), (b) Mg-saponite (Si/Al ratio 7.89), and (c) ASA.

Table 3
Activity and selectivity towards the conversion of *n*-heptane to *i*-heptane

M[a]	Si/Al[b]	*T* (°C)/ 40%[c]	Y_{max} (%)/ C_{max} (°C)[d]	*T*-profile[e] (°C)
Co	5.67	258	12/∼90	180–380
Co	7.89	250	15/40–65	180–380
Co	12.3	264	12/∼90	180–380
Mg	7.89	286	64/78	180–380
Mg	12.3	274	64/78	180–380
Mg	5.67	278	77/83	400–200
Mg	7.89	287	77/83	400–200
Mg	12.3	291	70/82	400–200
Co/Mg (1:1)	7.89	278	∼10/∼82	200–400
Co/Mg (1:1)	7.89	323	45/78	400–200[f]
Ni/Mg (5:1)	7.89	278	∼8/55	200–400
Ni/Mg (5:1)	7.89	323	45/81	400–200[f]

[a] Octahedral cation in the saponite structure.

[b] Si/Al ratio in the saponite structure.

[c] Temperature at 40% conversion.

[d] Maximum i-C_7 yield/corresponding reaction temperature.

[e] Temperature profile of the reaction.

[f] After previous reaction and subsequent treatment at 400 °C for 4 h in H_2.

higher than the conversion of the Mg-saponite with the same Si/Al ratio. The difference in temperature at 40% conversion is 36 °C. Under the conditions of the pretreatment (2 h at 400 °C within 30 bar of H_2), reduction of cobalt in the clay structure must have taken place. Cracking of *n*-heptane on the surface of metallic Co particles is most likely.

Both the (reduced) Co-saponite and the Mg-saponite are considerably more active than the commercial ASA catalyst. The difference in temperature at 40% conversion between the ASA and Mg-saponite is about 55 °C in favour of Mg-saponite. The hydro-isomerisation activity of a HZSM-5 zeolite is, however, considerably higher as compared with the synthetic saponites. Already at approximately 210 °C the conversion amounts to 40% with a HZSM-5 zeolite. This higher activity of the HZSM-5 zeolite can be explained by the higher (Brønsted) acid strength of this kind of catalyst as compared with saponites [30]. The yields versus conversion curves (Fig. 4) confirm the presence of larger metallic Co in Co-saponites. Although the activity of Co-saponite is high, the selectivity for *i*-heptane is low: approximately 15% i-C_7 yield between 40 and 65% conversion. The selectivity profile of Mg-saponite is almost the same as that of the ASA. The i-C_7 yields of both the ASA and Mg-saponite increase linearly with the conversion, resulting in an i-C_7 selectivity of 85–90%. In case of Mg-saponite the high selectivity is maintained up to 80% conversion. At higher conversions the i-C_7 yield drops because of the catalytic cracking of *n*-heptane at these temperatures over the acid sites of the Mg-saponite.

The results of the catalytic measurements of the above-mentioned samples and some other saponite samples are listed in Table 3. It is remarkable that the Si/Al ratio of the saponites does not show a consistent effect in the catalytic performance. Mg-saponite exhibits a slightly higher activity with decreasing Si/Al ratio at decreasing temperatures. However, subsequent measurements at increasing temperatures results in an opposite behaviour. Co-saponites do not exhibit any trend. The presence of Ni or Co in saponites with a mixed-metal octahedral sheet leads to a metallic behaviour similar to that of Co-saponite at increasing temperatures. It is interesting to note that after measuring from 200 to 400 °C and subsequent treatment in H_2 at 400 °C for 2 h, the reaction profile from 400 to 200 °C is totally different from the profiles measured earlier with the saponites containing exclusively Ni or Co. Although the resulting activities are considerably lower, the selectivities have increased a great deal. This can be attributed to the accumulation of carbon on the metallic particles during the process. Because of this carbon deposition the Ni or Co particles can no longer participate in the cracking of *n*-heptane, resulting in an increase of the selectivity for *i*-heptane due to the catalytic activity of the remaining (Lewis) acid sites.

Ni- and Co-containing synthetic mica-montmorillonites (SMM) show a very high activity and selectivity for the hydro-isomerisation of *n*-hexane [11,12]. Although the Co-containing saponite also displays a high activity in our study, the selectivity is low. The catalytic activity and selectivity of Ni-containing saponites are both low. Apparently the partial reduction of Ni/Co in the dioctahedral sheet of SMM results in an increase in the number of acid sites, whereas partial reduction of Ni or Co present in the trioctahedral sheet of the saponites of this study decreases the number of acid sites. The effect of reduction on the number of acid sites within mica-montmorillonites is attributed to a significant fraction of the nickel or cobalt present at interlayer positions. Reduction of metal ions at interlayer positions leads to protons neutralising the negative charge of the clay layers. Reduction of the metal ions present within the octahedral sheets brings about reaction of two hydroxyl groups and two oxygen ions per three nickel ions with hydrogen to water. A collapse of the clay structure results because of the removal of oxygen as water. It is interesting to note that Na^+- and Ce^{3+}-exchanged natural montmorillonites do not show catalytic activity for the conversion of *n*-heptane into *i*-heptane [37]. The authors observed that pillaring the montmorillonites with Al_{13} complexes gives rise to a 40% *n*-heptane conversion at about 335 °C, thus at a considerably lower temperature than we observed with Mg-saponite. The WHSV in their study is lower than that used in this study. Even pillaring with large complexes of Ce and Al did not result in a better activity than that obtained with our Mg-saponite [38].

3.3. Friedel–Crafts alkylation of benzene with propylene to cumene

A comparison of the results obtained with the commercial SPA catalyst and those obtained with a synthetic Zn-saponite with interlayer Al^{3+} in the Friedel–Crafts alkylation of benzene with propylene is presented in Table 4. The addition of some water to the feed was necessary when the SPA catalyst was used, in order to activate this catalyst. It can be seen that with 1.5 wt% Zn-saponite the conversion at 160 °C is 99% after 0.25 h. Decreasing the amount of saponite used at 160 °C from 1.5 to 0.2 wt% results in a slight drop in conversion from 99 to 87%. The selectivity does not differ much. When the SPA catalyst is used under these conditions (0.2 wt% at 160 °C for 0.25 h), the catalytic activity is reduced to almost zero. The substantially better catalytic performance of the synthetic Zn-saponite is therefore striking. Removing the SPA catalyst from the autoclave after the reaction was almost impossible. A layer of material was strongly attached to the reactor wall. Synthetic saponite, on the contrary, can be removed from the autoclave without problems. The influence of the state of hydration of the Zn-saponite on the catalytic performance is presented in Fig. 5. The presence of water in the feed results in a completely deactivated Zn-saponite. Obviously the acid sites are blocked by water and are, therefore, inactive for the reactants. Increasing the drying temperature to 120 °C results in a strong increase in the activity to 87%. A further increase in the pretreatment temperature to 300 °C causes the activity to decrease to 60%. This catalytic behaviour is in accordance with the acid properties of the Zn-saponites [30]. Although the temperatures are not entirely the same, the Zn-saponite with interlayer Al^{3+} shows a much higher acidity when dried at 150 °C than when calcined at 350 °C. The increase in acidity at 150 °C as compared with 350 °C is probably caused by the formation of Brønsted acid sites due to the dissociation of water within the interlayer by the exchangeable Al^{3+} cations. The selectivity of the samples is not affected by the amount of water present in the sample. The selectivity for cumene varies between 74 and 83%.

Table 4
Comparison between a commercial SPA catalyst with an Al^{3+}-exchanged Zn-saponite for the Friedel–Crafts alkylation of benzene with propylene to cumene

Sample	Wt% catalysts	B/P ratio[a]	*T* (°C)/ time (h)[b]	Conversion (%)	Selectivity (%)
SPA	1.5	8.7	190/2	85	80
Zn-sap[c]	1.5	7.7	190/2	99	83
Zn-sap[c]	1.5	7.1	160/0.25	99	80
Zn-sap[c]	0.2	6.8	160/0.25	87	74
SPA	0.2	7.7	160/0.25	0.3	100

[a] Initial benzene/propylene molar ratio.
[b] Reaction temperature/reaction time.
[c] Saponite Si/Al ratio = 39.0.

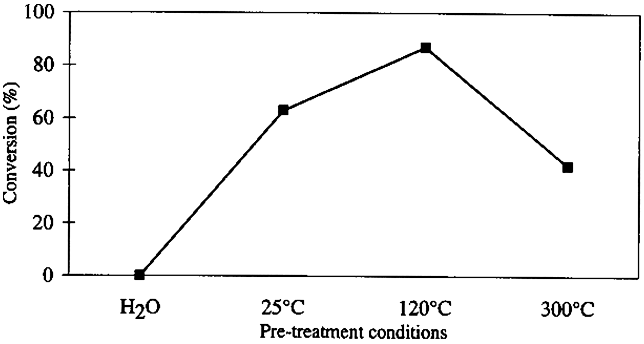

Fig. 5. The influence of the hydration state of Zn-saponite (Si/Al ratio 7.89) on the catalytic activity. Catalyst conversion 0.2 wt%, H_2O means wet saponite sample. Reaction conditions: temperature 160 °C, duration 0.25 h, benzene/propylene molar ratio ∼ 7.

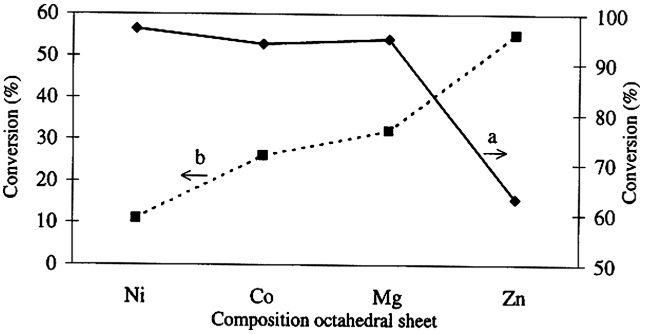

Fig. 6. The influence of the composition of the octahedral sheet (Ni^{2+}, Co^{2+}, Mg^{2+}, and Zn^{2+}) with (a) H^+- and (b) Al^{3+}-exchanged saponites (Si/Al ratio 7.89) on the catalytic performance. H^+-saponites: 1.5 wt% catalyst at 190 °C and 2 h, Al^{3+}-saponites: 0.2 wt% catalyst at 160 °C for 0.25 h.

Up to this point, the catalytic performance of saponites with Zn^{2+} in the octahedral sheets has been described. In Fig. 6 the effect of the type of octahedral and the interlayer cation on the catalytic performance is shown. Reactions using H^+-exchanged Ni-, Mg-, and Co-saponites (1.5 wt%) all show a very high conversion of about 95%, whereas the activity of the Zn-saponite is considerably lower (63%). As mentioned before, H^+-exchanged saponites exhibit Lewis acidity almost exclusively. It can thus be concluded that the alkylation of benzene with propylene is due to Lewis, but also to Brønsted, acid sites, as indicated by the Al^{3+}-exchanged Zn-saponites mentioned earlier. It is likely that in the case of H^+-exchanged saponites the interlayer space is too small to permit catalytic reactions, especially when the proton has migrated through the hexagonal cavities of the tetrahedral sheet, as suggested by Vogels et al. [30]. In that case the catalytic reactions can only take place at the external surface of the clay particles. As shown by Vogels et al. [28], the specific surface area of Zn-saponite is considerably lower than those of the saponites with Mg^{2+}, Ni^{2+}, or Co^{2+} as cation in the octahedral sheet, which accordingly results in a lower catalytic activity.

Al^{3+}-exchanged saponites exhibit behaviour opposite that of H^+-exchanged saponites. Al^{3+}-exchanged Zn-saponite (0.2 wt%) shows the highest activity, followed by Mg-, Co-, and Ni-saponite. These results are in good agreement with the pyridine-TPD results described by Vogels et al. [30]. In that work the highest acidity was also observed with (Al^{3+}-exchanged) Zn-saponite, followed by Mg- and Ni-saponites. These results may be partly explained by the high degree of stacking in Zn-saponites as compared with that of other saponites. Al^{3+} is mainly situated between two adjacent clay platelets and is predominantly responsible for the acidic properties. This hypothesis is not entirely true, because Co-saponite displays the second highest extent of stacking, but its catalytic performance is considerably lower than the hardly stacked Mg-saponite. Apparently the nature of the octahedral cation affects the acidic properties as well [30]. The high alkylation activity of catalysts containing Zn^{2+} has also been mentioned in the literature [22,26]. The selectivity for cumene ranges from 75 to 94% for all of the above-mentioned saponite samples. A clear relation between the type of octahedral or interlayer cation and the selectivity could not be observed.

The effect of the Si/Al ratio in Zn-saponite on the catalytic performance is presented in Fig. 7. Just as in the experiments described above, saponites exchanged with H^+ or Al^{3+} exhibit behaviours that are the opposite of each other. With H^+-exchanged Zn-saponite, the catalytic activity generally increases with decreasing Si/Al ratio. In other words, an increase in the amount of isomorphous substitution of Si by Al results in an increase in the number of acid sites at the external surface and correspondingly to an enhanced catalytic activity. The deviating behaviour of Al^{3+}-exchanged saponites is not fully understood. It can be suggested that a low amount of Al^{3+} in the tetrahedral sheet results in a low number of acid sites, but with a relatively strong acidity, according to the next nearest neighbour (NNN) effect, as indicated in zeolites. However, when this NNN theory is applied to saponites, the acid strength of the sites of a saponite with a Si/Al ratio of 7.89 will probably not differ from the acid strength of saponites with a Si/Al ratio of 39.0, but the number of acid sites is considerably higher, which should result in a higher catalytic activity. It may be concluded that at low Si/Al ratios the interlayer is largely occupied by exchangeable Al^{3+}, which impedes the diffusion of reactants and products into the interlayer space, resulting in a lower activity. However, this hypothesis can only be verified by more research. The selectivities we measured varied between 74 and 84% without any obvious trend.

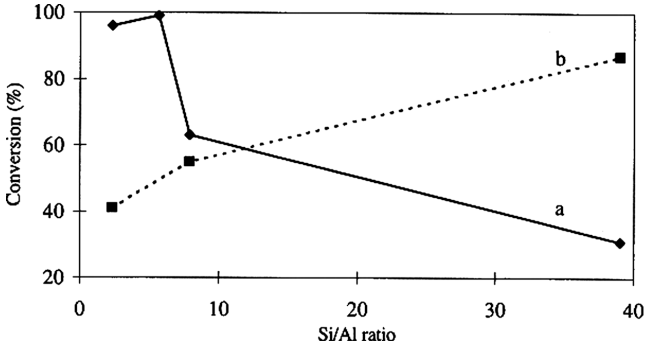

Fig. 7. The influence of the Si/Al molar ratio in (a) H^+- and (b) Al^{3+}-exchanged Zn-saponites on the catalytic performance. H^+-saponites: 1.5 wt% catalyst at 190 °C and 2 h, Al^{3+}-saponites: 0.2 wt% catalyst at 160 °C for 0.25 h.

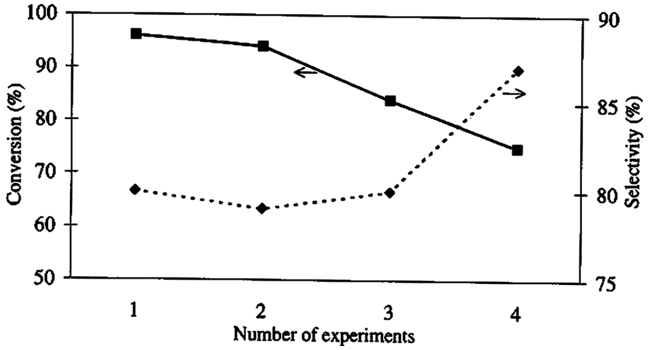

Fig. 8. Re-use experiments with an Al^{3+}-exchanged Zn-saponite (Si/Al ratio 7.89). Benzene/propylene molar ratio ~ 8, catalyst concentration 1.0 wt%, temperature 160 °C, reaction time 0.5 h.

We investigated the deactivation of an Al^{3+}-exchanged Zn-saponite with a Si/Al ratio of 39.0 by re-using the same sample in the alkylation reaction three times (Fig. 8). A decrease in the conversion from 96 to 75% was observed between the first and third experiments, coinciding with an increase in the selectivity from 80 to 87%. The deactivation is possibly due to the deposition of reaction products on the (strongest) acid sites. In other (single) alkylation experiments performed in this study, approximately 2–3 wt% carbon was measured to be deposited on the samples. This carbon possibly originates from polyalkylated products. The remaining weaker acid sites apparently favour the reaction towards cumene. As indicated earlier, the catalytic performance of Zn-saponites in the alkylation of benzene with propylene is far more favourable than that of the

Table 5
Selectivity towards p-, o-, and m-diisopropylbenzene (DIPB) for Al^{3+}-exchanged Zn-saponite (Si/Al ratio = 39.0, dried at 120 °C)

Wt% catalyst	T[a] (°C)	Time[b] (h)	Conversion (%)	p-DIPB (%)	o-DIPB (%)	m-DIPB (%)
1.5	190	2	99	47	50	3
1.5	160	0.25	98	47	36	17
0.2	160	0.25	87	49	35	16

[a] Reaction temperature.
[b] Reaction duration.

commercial SPA catalyst. Recently a new cumene production catalyst was developed by Dow Chemical based on a dealuminated mordenite catalyst [39]. Good alkylation performances by β zeolites have also been described. Unfortunately, because of differences in experimental setup, the results of these studies cannot be compared to the results with the synthetic saponites. Meima et al. [39] mentioned an interesting feature concerning the second most important product, DIPB: although m-DIPB is thermodynamically the most favoured isomer, the p-DIPB isomer was formed preferentially, and the o-isomer was hardly present. They concluded that this shape selectivity originated from the special porous character of the dealuminated zeolites. A similar shape selectivity was mentioned by Keading [40], who used a zeolite ZSM-12. When an Al^{3+}-exchanged Zn-saponite is measured, a strong selectivity for m-DIPB and, in contrast to other studies, the o-DIPB isomer is found, whereas the p-DIPB is hardly present (Table 5). Especially at higher reaction temperatures and longer duration, p- and o-DIPB are formed almost exclusively. Apparently the texture of the synthetic saponite is such that p- and o-DIPB are preferentially formed despite the fact that the m-DIPB isomer is thermodynamically most favoured.

4. Conclusions

Because of their acidic nature, synthetic saponites catalyse the cracking of n-dodecane, the hydro-isomerisation of n-heptane, and the Friedel–Crafts alkylation of benzene with propylene. As was to be expected from our earlier work (Vogels et al., 2004), the compositions of the octahedral sheet and the tetrahedral sheet and the type of exchangeable cations largely influence the catalytic properties of the saponites in all three reactions. Differences in the texture of the various saponites can play an important role. In the catalytic cracking of n-dodecane the Mg-saponite was far more active than saponites with other cations in the octahedral sheet. The higher activity probably is related to the higher specific surface area of this sample. An optimum in activity was observed for saponites with a Si/Al ratio of 7.89. The high selectivity for olefins of Co-saponite was striking. The saponites are considerably more active in the hydro-isomerisation of n-heptane than are commercial ASA and the pillared clay material mentioned in the literature. The HZSM-5 zeolite, however, was considerably more efficient in the hydro-isomerisation reaction. Although the Co-saponite turned out to be more active than Mg-saponite, the selectivity for i-heptane was very low. Saponites were also active in the Friedel–Crafts alkylation of benzene with propylene at relatively low temperatures (160 °C). The shape selectivity for p- and o-DIPB was remarkable. It was indicated that the amount of water in the system largely affects the catalytic properties of the saponites. Too much water results in a blocking of the active sites. The synthetic saponites were far more active than the commercial SPA catalyst. It is generally known that the application of the SPA catalyst has some serious drawbacks with respect to corrosion and environmental damage. Furthermore, the SPA catalysts are difficult to remove from the reaction vessel and cannot be re-used. The synthetic clay minerals are harmless with respect to the environment, are easy to handle, are easy to remove from the reaction vessel, and are re-useable. The catalytic performance in the alkylation reaction of benzene with propylene of the synthetic saponites is such that it can compete with the SPA catalyst. It can be concluded that the catalytic alkylation reaction is a good example in which environmentally friendly synthetic clay minerals are possibly able to replace the SPA catalyst.

References

[1] H.W. Bondt, J.R. Deiman, P. van Troostwyk, A. Lowrenberg, Ann. Chim. Phys. 21 (1797).
[2] W.P.J. Hettinger, Appl. Clay Sci. 5 (1991) 445.
[3] J.P. Rupert, W.T. Granquist, T.J. Pinnavaia, in: A.C.D. Newman (Ed.), Chemistry of Clays, Clay Minerals, vol. Monograph No. 6, Mineralogical Society, London, 1987, p. 275.
[4] E. Houdry, W.F. Burt, A.E. Pew Jr., W.A. Peters Jr., Nat. Pet. News 37 (1938) R570.
[5] T.J. Pinnavaia, Science 220 (1983) 365.
[6] A. Vaccari, Appl. Clay Sci. 14 (1999) 161.
[7] J. Monnier, J.-P. Charland, J.R. Brown, M.F. Wilson, Proc. 10th Int. Conf. Catal., 1993, p. 1943.
[8] J.T. Kloprogge, J. Porous Mater. 5 (1998) 5.
[9] Z. Ding, J.T. Kloprogge, R.L. Frost, G.Q. Lu, H.Y. Zhu, J. Porous Mater. 8 (2001) 273.
[10] F.E. Condon, in: P.H. Emmett (Ed.), Catalysis, vol. 4, Reinhold, New York, 1958, p. 2091.
[11] J.J.L. Heinerman, I.L.C. Freriks, J. Gaaf, G.T. Pott, J.G.F. Coolegem, J. Catal. 80 (1983) 145.
[12] K.H.W. Robschlager, C.A. Emeis, R.A. van Santen, J. Catal. 86 (1984) 1.
[13] R.A. van Santen, K.H.W. Robschlager, C.A. Emeis, in: R.K. Grasselli, J.F. Brazdil (Eds.), in: Solid State Chemistry in Catalysis, ACS Symp. Series, vol. 279, American Chemical Society, Washington, D.C., 1985, p. 275.
[14] D. Jiang, T. Sun, Z. Liu, E. Min, M. He, in: Proc. 9th Int. Zeolite Conf. 1992, Montreal, 1993, p. 631.
[15] J.A. Ballantine, in: R. Setton (Ed.), Chemical Reaction in Organic, Inorganic Constrained Systems, Reidel, Dordrecht, 1986, p. 197.
[16] J.M. Adams, Appl. Clay Sci. 2 (1987) 309.
[17] D.R. Brown, Geol. Carp., Series Clays (Bratislava) 45 (1994) 45.
[18] B. Chiche, A. Finiels, C. Gauthier, P. Geneste, J. Mol. Catal. 42 (1987) 229.

[19] K. Pitchumani, A. Pandian, J. Chem. Soc., Chem. Commun. (1990) 1613.

[20] C.N. Rhodes, D.R. Brown, Catal. Lett. 24 (1994) 285.

[21] P.D. Clark, A. Kirk, R.A. Kydd, Catal. Lett. 25 (1994) 163.

[22] P.D. Clark, A.P. Kybett, D.J. Macquarrie, S.J. Barlow, P. Landon, J. Chem. Soc., Chem. Commun. (1989) 1353.

[23] A. Cornelis, P. Laszlo, Synthesis (1985) 909.

[24] K. Urabe, H. Matsuoka, Y. Izumi, Europacat-II, Maastricht, 3–8 September 1995, p. 418.

[25] M.I. Knutsen, J.L. McAtee, Clays Clay Miner. 21 (1973) 19.

[26] V. Luca, L. Kevan, C.N. Rhodes, D.R. Brown, Clay Miner. 27 (1992) 515.

[27] K. Urabe, M. Koga, Y. Izumi, J. Chem. Soc., Chem. Commun. (1989) 807.

[28] R.J.M.J. Vogels, J.T. Kloprogge, J.W. Geus, Amer. Mineral. (2004), Synthesis, characterisation of saponite clays, ’in press.

[29] R.J.M.J. Vogels, J.T. Kloprogge, J.W. Geus, Am. Miner. (2004), Synthesis and characterisation of saponite clays: part 2, Thermal stability, in press.

[30] R.J.M.J. Vogels, J.T. Kloprogge, J.W. Geus, Appl. Catal. A (2004), Brønsted, lewis acidity of synthetic saponites, stevensites: effects of substitution, cation exchange, hydration state, submitted for publication.

[31] A.J. van Dillen, J.W. Geus, L.A.M. Hermans, J. Van der Meijden, Proc. 6th Int. Conf. Catal. 11 (1977) 677.

[32] A. Corma, P.J. Miguel, A.V. Orchilles, Appl. Catal. A 117 (1994) 29.

[33] J. Meusinger, H. Vinek, J.A. Lercher, J. Mol. Catal. 87 (1994) 263.

[34] E. Dempsey, J. Catal. 33 (1974) 497.

[35] E. Dempsey, J. Catal. 39 (1975) 155.

[36] R.J. Mikovsky, J.F. Marshall, J. Catal. 44 (1976) 170.

[37] F. González, C. Pesquera, I. Benito, S. Mendioroz, G. Poncelet, J. Chem. Soc., Chem. Commun. (1992) 491.

[38] E. Booij, J.T. Kloprogge, J.A.R.v. Veen, Clays Clay Miner. 44 (1996) 774.

[39] G.R. Meima, M.J.M. van der Aalst, M.S.U. Samson, J.M. Garces, J.G. Lee, in: Proc. 9th Int. Zeolite Conf., Montreal, 1992, vol. 2, Butterwort-Heinemann, Boston, 1993, p. 327.

[40] W.W. Keading, J. Catal. 120 (1989) 409.